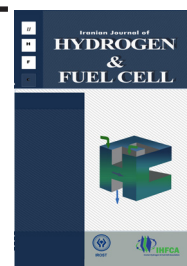


Iranian Journal of Hydrogen & Fuel Cell

IJHFC

Journal homepage://ijhfc.irost.ir



Application of Pd-Substituted Ni-Al layered double hydroxides for the hydrogen evolution reaction

Ali Reza Madram* , Navid Zandi Atashbar

Faculty of Chemistry and Chemical Engineering, Malek-Ashtar University of Technology, Tehran 15875-1774, IRAN

Article Information

Article History:

Received:

04 March 2016

Received in revised form:

21 May 2016

Accepted:

28 May 2016

Keywords

Hydrogen evolution reaction

(HER)

Layered double hydroxide (LDH)

Carbon black

Pd substitution.

Abstract

Production of hydrogen from electrochemical water splitting is known as a green method of fuel production. In this work, electrocatalytic hydrogen evolution reaction (HER) was investigated for newly prepared layered double hydroxides (LDH) in acidic solution. NiAl LDH/CB (carbon black) LDH was monitored using x-ray diffraction (XRD), Fourier transform infrared (FT-IR) spectroscopy, and scanning electron microscopy (SEM). The substitution of nickel ions with palladium ones was recorded using Energy dispersive X-ray spectroscopy (EDX). Moreover, the NiAl-LDH/CB and palladium substituted LDH were examined for the HER at different times of substitution. The modified NiAl LDH/CB/Pd/GCE (glass carbon electrode) represented low overpotential of -0.55 V (vs. Ag/AgCl), Tafel slope of 125 mV/dec, charge transfer coefficient of 0.47, exchange current of 2.56 μA , as well as excellent long-term stability. Moreover, the substitution effect of palladium ions on the modification of prepared LDH GCE was satisfactorily studied for the HER in 0.5 mol L⁻¹ H₂SO₄ using electrochemical impedance spectroscopy (EIS).

1. Introduction

Hydrogen as a clean fuel compared to fossil fuels has received considerable attention, particularly when hydrogen is generated using green techniques such as electrochemical and photo electrochemical water splitting [1-4]. The water-splitting reaction can occur via two half reactions: the oxygen evolution reaction (OER) and the hydrogen evolution reaction (HER) [5]. The HER is a cathodic half-reaction of water

electrolysis and it demands an active catalyst with lower overpotential for facile evolution of hydrogen, like Pt [6]. Nonetheless, high price and limited sources of Pt are other serious barriers for the commercialization of water electrolysis. Hence, to achieve this aim the development of cost-effective, highly active, and stable electro catalysts, such as the transitional metal chalcogenides and nano-composite materials, has been studied for the HER [7,8]. Recently, layered double hydroxides (LDHs), such as anionic clays, have been

*Corresponding Author's Tel.: +98 21 22549213; Fax: +98-21-22962257
E-mail address: Ar.madram@gmail.com (A.R. Madram).

attended by researchers due to their usability in various applications such as catalyst, adsorbent, and nano based materials [9-15]. LDHs can be derived by partly substituting cations, such as Al^{3+} , Fe^{3+} , or Ni^{2+} , for Mg^{2+} in the brucite structure of $\text{Mg}(\text{OH})_2$. The replacement of di-valent cations with tri-valent ones creates a positively charged layer on the LDHs, which can be balanced by anions or anionic complexes located in the inter-layer region. Hence, a wide range of LDH compositions have been created by the general formula $[\text{M}^{2+}_{1-x}\text{M}^{3+}_x(\text{OH})_2][\text{A}^{n-}]_{x/n} \cdot y\text{H}_2\text{O}$ (M^{2+} and M^{3+} are, respectively, the di- and tri- valent cations in the octahedral positions within the hydroxide layers; A^{n-} is an exchangeable interlayer anion). Thus, cationic and anionic replacements result in various compositions for layered double hydroxides [16-18]. Moreover, this variation of LDH composition can be increased by using carbon-based materials in alkaline media to form new LDHs with improved properties [19,20].

In this work, carbon black (CB) was employed for this objective and we reported a new electrocatalysts for the HER, composed of NiAl-LDH/CB, in acidic medium. Furthermore, the effect of replacement of nickel and aluminum ions with palladium ions on its electrocatalytic activity toward the HER was studied by linear sweep voltammetry (LSV), steady-state polarization Tafel curves and electrochemical impedance spectroscopy (EIS) techniques.

2. Experimental

2.1 Materials and Apparatus

Nickel nitrate ($\text{Ni}(\text{NO}_3)_2 \cdot 6\text{H}_2\text{O}$), aluminum nitrate ($\text{Al}(\text{NO}_3)_3 \cdot 9\text{H}_2\text{O}$), sodium hydroxide (NaOH), sulfuric acid (H_2SO_4), and palladium sulfate dehydrate ($\text{PdSO}_4 \cdot 2\text{H}_2\text{O}$) were purchased from Merck and CB was purchased from Lexcel (99%, mesh 325). All other reagents were of analytical grade and used without further purification. The water used throughout all experiments was twice distilled deionized water. The Fourier transform infrared spectra were recorded on an FT-IR Spectrometer (Jasco, FT/IR-680 Plus). The

morphology of LDHs was characterized by a field emission scanning electron microscope (FE SEM) (HITACHIS-4160) and energy dispersive X-ray spectra (EDX) were recorded with a Philips XL30 instrument. X-ray diffraction (XRD) analyses were carried out with a Bruker D8 Advance X-ray diffractometer using $\text{Cu-K}\alpha$ radiation. All electrochemical measurements were performed with an Autolab electrochemical analyzer, model PGSTAT-30 Potentiostat/Galvanostat (Eco-Chemie, Netherlands) and controlled by a microcomputer. Data were acquired and processed using the GPES computrace software 4.9.007. The Tafel plots were recorded galvanostatically (45 s after a constant current application) at cathodic current densities ranging from $j = -100 \text{ mA cm}^{-2}$ to $j = -1 \text{ }\mu\text{A cm}^{-2}$. At the steady state, the electrode potentials were recorded for iR drop, determined by the EIS method at various electrode potentials. The EIS measurements were recorded with a frequency range of 0.1 Hz to 10 kHz and the amplitude wave potential of 5 mV. All electrochemical experiments were carried out at room temperature and air atmosphere using a conventional three-electrode system with a modified glassy carbon electrode (GCE) as the working electrode, a Pt rod as the auxiliary electrode, and an $\text{Ag}/\text{AgCl}/3.0 \text{ mol L}^{-1} \text{ KCl}$ as the reference electrode. The electrocatalytic activity for the investigated LDH catalysts toward the HER was tested in $0.5 \text{ mol L}^{-1} \text{ H}_2\text{SO}_4$ solution.

2.2 Preparation of NiAl-LDH/CB

For the synthesis of the NiAl-LDH/CB, 0.581 g $\text{Ni}(\text{NO}_3)_2 \cdot 6\text{H}_2\text{O}$ and 0.375 g $\text{Al}(\text{NO}_3)_3 \cdot 9\text{H}_2\text{O}$ were added into 30.0 mL deionized water under vigorous stirring at room temperature and nitrogen atmosphere. The pH of the reaction mixture was adjusted to 8.5 by the addition of NaOH solution (Sample 1). Separately, carbon black with the mass ratio of 1.5 against Ni^{2+} was dispersed in the alkaline solution in an ultrasonic bath for 30 min (Sample 2). Sample 1 was then added to Sample 2 and stirred for 30 min at 70 °C, followed by dispersing under the ultrasonic waves for 1 h. Afterward, the resulting precipitate was separated by

centrifugation at 4000 rpm for 10 min, then washed three times with deionized water and dried in a vacuum oven at 50 °C for 2 h.

2.3 Preparation of NiAl-LDH/CB/GCE and NiAl-LDH/CB/Pd/GCE

The GCE, with a diameter of 1.6 mm, was pretreated by polishing with alumina slurry, rinsed with twice distilled water, and immersed in the water-ethanol mixture in an ultrasonic bath for 3 min. 2.0 mg NiAl-LDH/CB was dispersed in 800 μ L water-ethanol using the ultrasonic bath for 2 min and then 10 μ L of the suspension was dropped on the pretreated GCE and dried at room temperature. Afterward, the Nafion was coated by dropping 3 μ L of 1.0% Nafion solution on the NiAl-LDH/CB/GCE surface and drying at room temperature. After Nafion coating, the NiAl-LDH/CB/Pd/GCEs were prepared by immersing the NiAl-LDH/CB/GCE in 5 mmol L⁻¹ of palladium solution for various times (0, 10, 20, 30, 60, 90 and 120 min). Before the electrochemical analysis, the modified electrode was rinsed with distilled water, and then dried at room temperature.

3. Results and discussion

3.1. Electrode composition and surface morphology

The synthesized NiAl-LDH/CB was evaluated by three techniques, XRD analysis, FT-IR spectroscopy and FE-SEM. Powder XRD patterns for the carbon black and synthesized NiAl-LDH/CB were recorded in 2 θ range of 10–70° with CuK α radiation, as shown in Fig. 1. According to pattern (a), the XRD of CB indicated two broadened peaks, assigned (002) and (101), due to its graphen layers which conform to what was reported previously in [21]. As indicated in Fig. 1b, the XRD pattern for the NiAl-LDH/CB sample showed seven peaks located at 11.0°, 23.2°, 34.7°, 39.1°, 46.9°, 61.7°, and 62.6°, corresponding to the multi-phases of NiAl-LDH, similar to what was reported elsewhere [22]. The sharp peak centered at 29.4° can also be

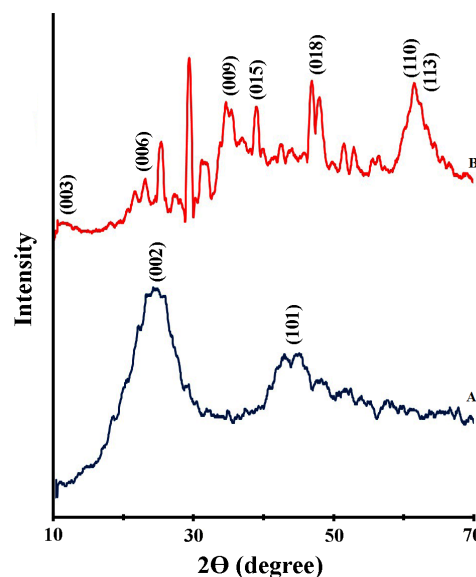


Fig. 1. Powder X-ray diffraction spectra (XRD) of carbon black (A) and NiAl-LDH/CB (B).

allocated to the Ni₃Al LDH structure. Non-assigned peaks can be referred to phase changes due to entrance of CB at inter-layer region. The synthesis of NiAl-LDH/CB was also monitored by FT-IR spectroscopy, as exhibited in Fig. 2. The FT-IR spectrum was plotted in the wavenumber range of 400–4000 cm⁻¹. Accordingly, the absorption bands of 1116.7, 1642.1, 1731.8, 2884.0, and 3444.2 cm⁻¹ corresponded respectively to C-O, C=C, C=O, C-H, and O-H showing that the carbon black was well located in the LDH structure. Moreover, the absorption band of 3444.2 cm⁻¹ can be assigned to OH group of metal hydroxide. The stretching mode of nickel and aluminum nitrate can be seen at 1379.8 cm⁻¹. The bands placed in the 400–900 cm⁻¹ range also corresponded to the metal-oxygen bands (M-O), as reported previously by Abdolmohammad-Zadeh and Kohansal [23]. As mentioned in the experimental section, the effect of palladium ion as a modifier in the HER was investigated by replacing the nickel ones with palladium ions. EDX spectra were recorded at different times of palladium replacement and shown in Fig. 3 for 0 (A), 60 (B) and 120 min (C). As shown in Fig. 3, the atomic percentages of Ni:Al:Pd were 69.8:30.2:0.0, 54.9:36.8:8.3 and 47.1:40.4:12.5 for replacement times of 0, 60 and 120 min, respectively.

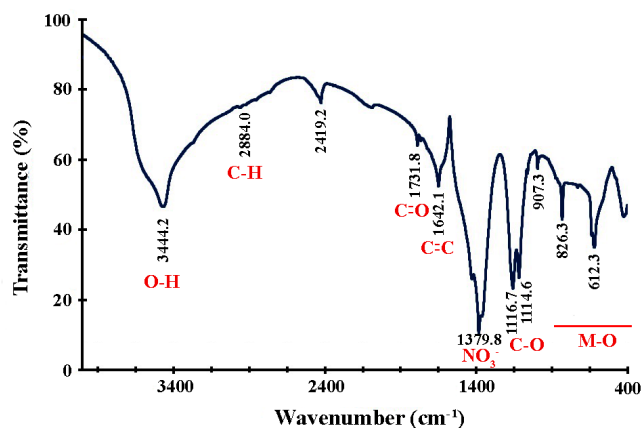


Fig. 2. Fourier transform infrared (FT-IR) spectrum of NiAl-LDH/CB, as KBr pellet.

Accordingly, the ratio of Ni to Al in the investigated LDHs was initially around 2.3 (0 min) while the

replacement of Pd led to a decrease this ratio to about 1.5 (60 min) and 1.2 (120 min). Fig. 4 displays

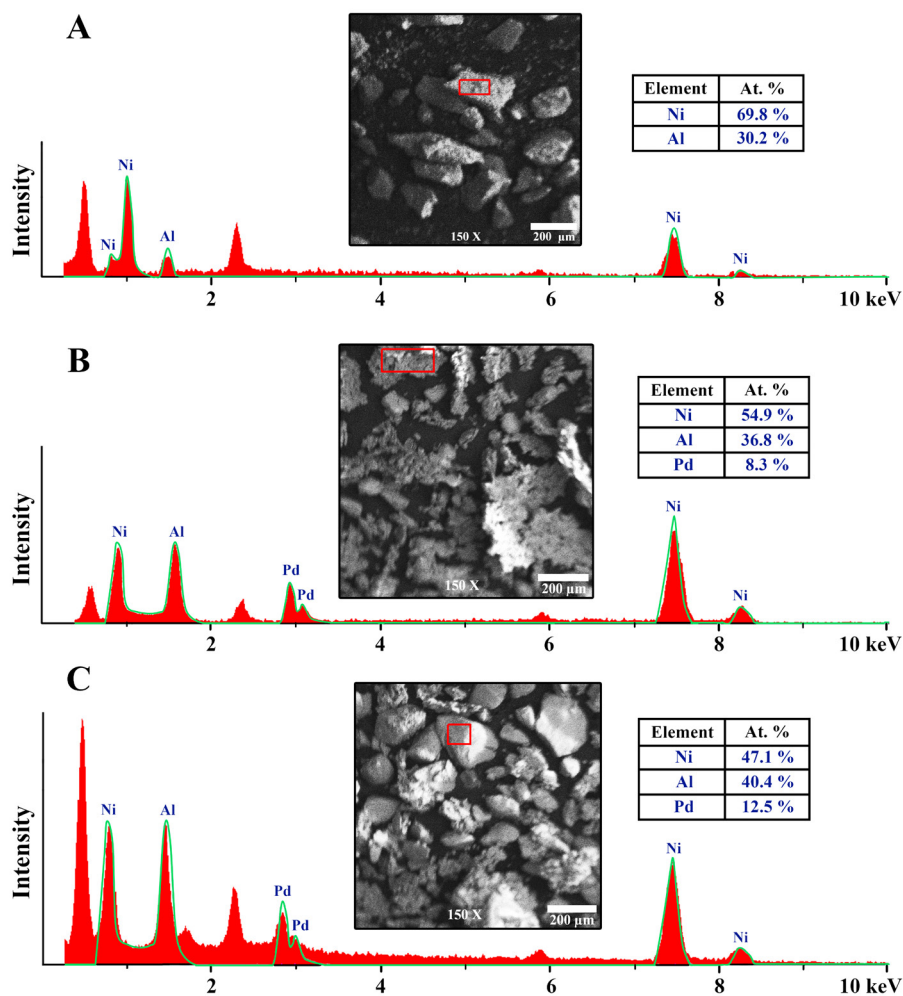


Fig. 3. EDX spectra of NiAl-LDH/CB (A), NiAl-LDH/CB/Pd after 60 min of Pd substitution (B) and after 120 min of Pd substitution (C).

the FE-SEM micrographs of carbon black (A) and NiAl-LDH /CB (B) and NiAl-LDH/CB/Pd (C). All images indicate the presence of separate graphen sheets in Fig. 4A and the LDH loaded by CB in the corresponding graph (Fig. 4B and C).

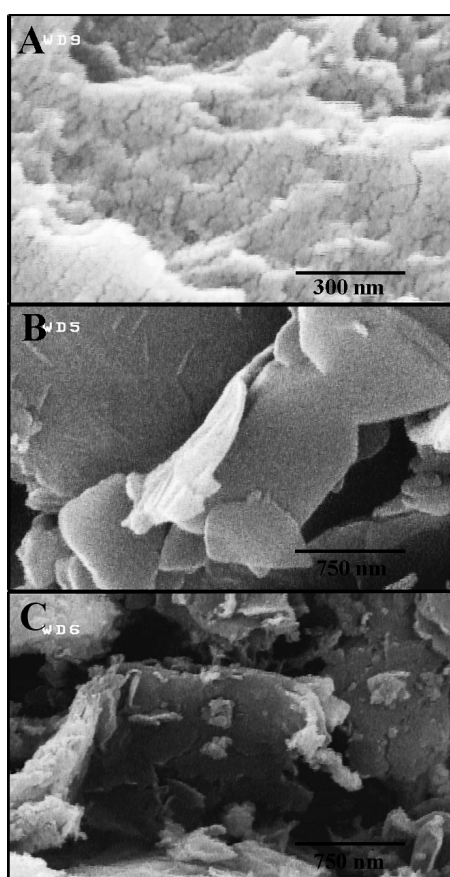


Fig. 4. FE-SEM images of carbon black (A), NiAl-LDH/CB (B), and NiAl-LDH/CB/Pd (C).

3.2. HER activity of the GCE modified by LDHs

The electrocatalytic activities of the investigated LDHs samples, i.e. NiAl LDH/CB and NiAl LDH/CB/Pd, were investigated for the HER in 0.5 mol L⁻¹ H₂SO₄ by LSV, Tafel curves and EIS methods using a 3 electrode setup. Fig. 5 shows the LSV behavior for the HER for GCE modified by NiAl LDH/CB and NiAl LDH/CB/Pd with different substitutions of Pd (replacement times of 0 to 120 min) at scan rate of 25 mV s⁻¹. This figure demonstrates the increasing HER activity increases as the substitution time increases until 120 min, when this activity became relatively

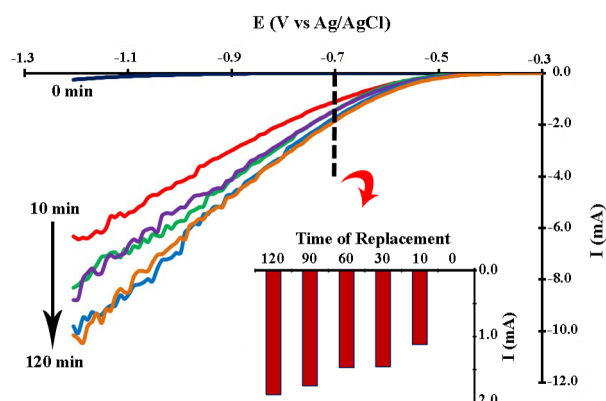


Fig. 5. HER activity of the modified LDH GCEs for different times of palladium replacement (0-120 min) using linear sweep voltammetry in 0.5 mol L⁻¹ H₂SO₄ at scan rate of 25 mV s⁻¹.

constant. Also, the inset of Fig. 5 shows the variation of the HER current at a constant potential ($E = -0.7$ V vs. Ag/AgCl) as a function of replacement time are shown. The practical application of the LDH for the HER relies on the long-term stability of the electrocatalyst [24]. It is remarkable that the HER activity increased until the 100th run and then remained stable even after the 500th run, confirming that the electrocatalysts NiAl-LDH/CB/Pd was useable for the HER as indicated in Fig. 6. Furthermore, it is shown that the increase of the potential scan could be resulted to increase of the HER currents.

Moreover, the steady-state polarization curves of the HER were studied to evaluate the electrocatalytic activities of the GCEs modified with the investigated

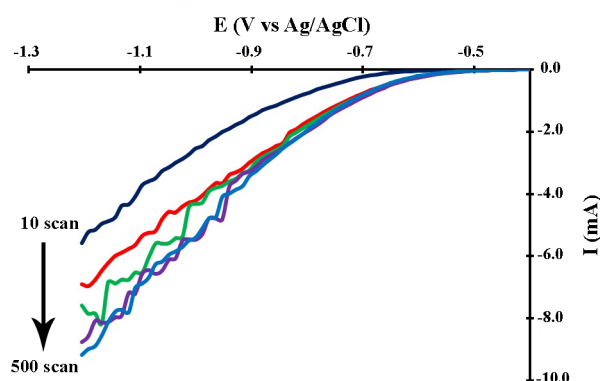


Fig. 6. The Stability of NiAl-LDH/CB/Pd for the HER to 500 scans of potential at scan rate of 25 mV s⁻¹.

LDHs. Fig. 7 indicates corresponding Tafel plots, when polarization curves were recorded in 0.5 mol L⁻¹ H₂SO₄ at a scan rate of 10 mV s⁻¹. Tafel plots on NiAl-LDH/CB/GCE and NiAl LDH/CB/Pd/GCE obviously suggested that the HER can be explained by the Tafel equation ($\eta = a + b \log i$), where i is the steady-state current, b is the Tafel slope, η is the overpotential, and a is the equivalent of the exchange current (i.e., $a = \log i_0$) [25]. Meanwhile, the Tafel and kinetic parameters for the HER at different electrodes were summarized in Table 1. These parameters were calculated taking into account the geometric surface area of the investigated LDHs. The Tafel curves for the NiAl-LDH/CB/GCE and NiAl LDH/CB/Pd/GCE showed only one Tafel slope in the whole range of studied potentials. Tafel slope can be a good estimation of the kinetic parameter of the charge transfer coefficient, α , ($b = 1/16.9\alpha$). Accordingly, increases in palladium substitution resulted in the effective charge transfer of the electron, i.e. the lower overpotential of hydrogen reduction. In other words, increases in the substitution time of Pd²⁺ led to larger α and i_0 (from 0.30 to 0.47 and from 1.10×10^{-2} μ A to 2.56 μ A, respectively). There were three suggested mechanisms for the HER in acidic media [25]:

1. $\text{H}_3\text{O}^+ + \text{e}^- \rightarrow \text{H}_{\text{ads}} + \text{H}_2\text{O}$ (Volmer reaction)
2. $\text{H}_{\text{ads}} + \text{H}_3\text{O}^+ + \text{e}^- \rightarrow \text{H}_2 + \text{H}_2\text{O}$ (Heyrovský reaction)
3. $\text{H}_{\text{ads}} + \text{H}_{\text{ads}} \rightarrow \text{H}_2$ (Tafel reaction)

If the Volmer reaction was the rate-determining step (rds), the Tafel slope would be 120 mV/dec, whereas the rate-determining steps of Tafel and Heyrovský reactions represented the Tafel slopes of 30 and 40 mV/dec, respectively. Hence, the HER activity of the

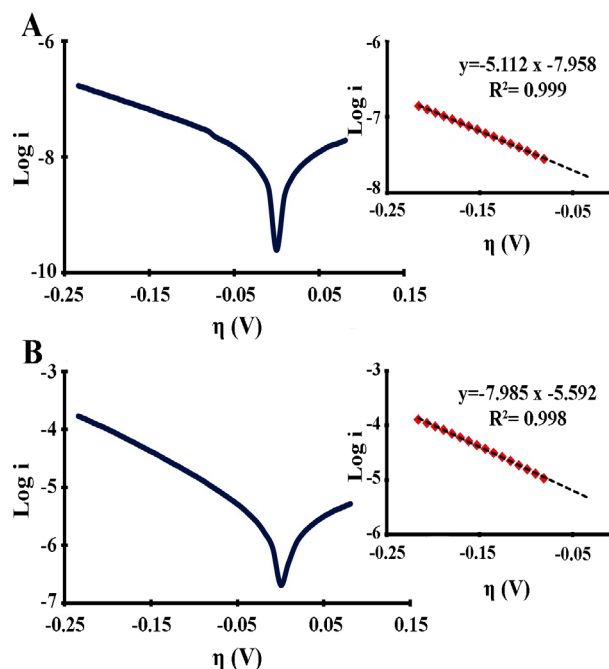


Fig. 7. Tafel plots for the HER at NiAl-LDH/CB/GCE (A) and NiAl-LDH/CB/Pd/GCE (B) at scan rate of 10 mV s⁻¹.

NiAl-LDH/CB/Pd suggested the Volmer reaction (with Tafel slope of 125 mV/dec) was rds at all studied Pd replacement times (Table 1). However, alone the Tafel curves studies are not enough to explain the kinetics of the HER. Thus, more precise information was obtained by the EIS. The Electrochemical impedance spectra were recorded at overpotential of -0.3 V. Fig. 8A indicates the Nyquist plots of three investigated electrodes of GCE (a), NiAl LDH/CB/GCE (b), and NiAl LDH/CB/Pd/GCE (c). Accordingly, the charge transfer resistance (R_{ct}) of the investigated electrodes clearly decreased when the electrode was modified (R_{ct} for GCE, NiAl LDH/CB/GCE and NiAl LDH/CB/Pd/GCE were about 15000, 2300 and

Table 1. Tafel and kinetic parameters for the HER at NiAl LDH/CB/GCE and NiAl LDH/CB/Pd/GCE surfaces.

Substitution time of Pd ²⁺ (min)	Charge transfer coefficient (α)	Exchange current (μ A)	Tafel slope (mV/dec)
0	0.30	$1.10(\times 10^{-2})$	195
10	0.42	1.53	140
60	0.47	1.27	125
90	0.47	2.39	125
120	0.47	2.56	125

670 Ω , respectively), as the corresponding recorded semicircle represented shorter diameter [26]. This performance was also confirmed when the EIS investigation was performed at different times of palladium substitution from 0 to 120 min, as showed in Fig. 8B (0 (a), 30 (b), 60 (c), 90 (d) and 120 min (e)). When further study of the operative potential was directed to more minor values, the Nyquist plots showed smaller semicircle because of more facile electron transfer at the NiAl LDH/CB/Pd/GCE (Fig. 8C: -10 (a), -15 (b), -20 (c), -25 (d), -30 (e), -35 (f) and -40 mV (g) vs. Ag/AgCl). Moreover, since the concentration of sulfuric acid was relatively high (0.5 mol L⁻¹) the diffusion-related part of plot was absent, so mass transfer was fast and the HER was controlled only by kinetic limitations. Similarity of electrocatalytic responses at all potentials represented

comparable mechanisms for the evolution of hydrogen.

4. Conclusion

NiAl-LDH/CB was synthesized and its electrocatalytic properties for the HER were improved by palladium substitution. The long-term stability of modified GCE represented a stable hydrogen evolution upto 500 cycles of voltammetry. The mechanism of HER was performed based on Volmer's reaction step due to the Tafel slope of 125 mV/dec, as well as charge transfer coefficient and exchange current of 0.47 and 2.56 μA , respectively. The EIS measurements of accelerated charge transferring confirmed the performance of HER at the modified NiAl-LDH/CB/Pd/GCE.

5. References

- [1] Zhang G, Lin B, Qiu Y, He L, Chen Y, Gao B. Highly efficient visible-light-driven photocatalytic hydrogen generation by immobilizing CdSe nanocrystals on ZnCr-layered double hydroxide nanosheets. *Int J Hydrogen Energ* 2015;40:4758-65.
- [2] Youn DH, Park YB, Kim JY, Magesh G, Jang YJ, Lee JS. One-pot synthesis of NiFe layered double hydroxide/reduced graphene oxide composite as an efficient electrocatalyst for electrochemical and photoelectrochemical water oxidation. *J Power Sources* 2015;294:437-43.
- [3] Xu D, Rui Y, Li Y, Zhang Q, Wang H. Zn-Co layered double hydroxide modified hematite photoanode forenhanced photoelectrochemical water splitting. *Appl Surf Sci* 2015 [Article in Press].
- [4] Shao M, Ning F, Wei M, Evans DG, Duan X. Hierarchical Nanowire Arrays Based on ZnO Core-Layered Double Hydroxide Shell for Largely Enhanced Photoelectrochemical Water Splitting. *Adv Funct Mater* 2014;24:580-6.
- [5] Bockris JOM, Potter EC. The Mechanism of the

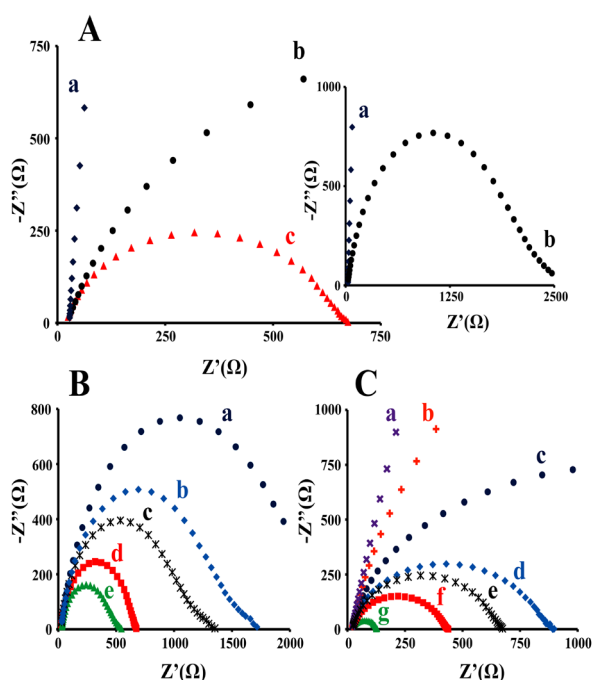


Fig. 8. Electrochemical impedance spectra recorded in the conditions: (A) at the surface of GCE (a), NiAl-LDH/CB/GCE (b), and NiAl-LDH/CB/Pd/GCE; (B) in different times of palladium substitution (0 (a), 20 (b), 60 (c), 90 (d), and 120 min (e)); and (C) at the surface of NiAl LDH/CB/Pd/GCE in 0.5 mol L⁻¹ H₂SO₄ applying different operative potentials (-10 (a), -15 (b), -20 (c), -25 (d), 30 (e), -35 (f), -40 mV vs Ag/AgCl (g)).

- Cathodic Hydrogen Evolution Reaction. *J Electrochem Soc* 1952;99:169–86.
- [6] Merki D, Hu X. Recent developments of molybdenum and tungsten sulfides as hydrogen evolution catalysts. *Energy Environ Sci* 2011;4:3878-88.
- [7] Zhang L, Xiong K, Nie Y, Wang X, Liao J, Wei Z. Sputtering nickel-molybdenum nanorods as an excellent hydrogen evolution reaction catalyst. *J Power Sources* 2015;297:413-8.
- [8] Akyüz D, Dinçer H, Özkaya AR, Koca A. Electrocatalytic hydrogen evolution reaction with metallophthalocyanines modified with click electrochemistry. *Int J Hydrogen Energy* 2015;40:12973-84.
- [9] Hasannia S, Yadollahi B. Zn–Al LDH nanostructures pillared by Fe substituted Keggin type polyoxometalate: Synthesis, characterization and catalytic effect in green oxidation of alcohols. *Polyhedron* 2015;99:260–5.
- [10] Morales-Mendoza G, Tzompantzi F, García-Mendoza C, López R, De la Luz V, Lee SW, Kim TH, Torres-Martínez LM, Gómez R. Mn-doped Zn/Al layered double hydroxides as photocatalysts for the 4-chlorophenol photodegradation. *Appl Clay Sci* 2015;118:38–47.
- [11] Laipan M, Zhu R, Chen Q, Zhu J, Xi Y, Ayoko GA, He H. From spent Mg/Al layered double hydroxide to porous carbon materials. *J Hazard Mat* 2015;300:572–80.
- [12] Wang S, Li Z, Lu C. Polyethyleneimine as a novel desorbent for anionic organic dyes on layered double hydroxide surface. *J Colloid Interf Sci* 2015;458:315–22.
- [13] Seftel EM, Niarchos M, Mitropoulos C, Mertens M, Vansant EF, Cool P. Photocatalytic removal of phenol and methylene-blue in aqueous media using TiO₂@LDH clay nanocomposites. *Catal Today* 2015;252:120–7.
- [14] Kim NH, Mishra AK, Kim DY, Lee JH. Synthesis of sulfonated poly(ether ether ketone)/layered double hydroxide nanocomposite membranes for fuel cell applications. *Chem Engin J* 2015;272:119–27.
- [15] Yadollahi M, Namazi H, Aghazadeh M. Antibacterial carboxymethyl cellulose/Ag nanocomposite hydrogels cross-linked with layered double hydroxides. *Int J Biol Macromol* 2015;79:269–77.
- [16] Paikaray S, Hendry MJ. Formation and crystallization of Mg²⁺–Fe³⁺–SO₄²⁻–CO₃²⁻-type anionic clays. *Appl Clay Sci* 2014;88-89:111-22.
- [17] Tan X, Fang M, Ren X, Mei H, Shao D, Wang X. Effect of Silicate on the Formation and Stability of Ni–Al LDH at the γ -Al₂O₃ Surface. *Environ Sci Technol* 2014;48:13138–45.
- [18] Li S, Wang H, Li W, Wu X, Tang W, Chen Y. Effect of Cu substitution on promoted benzene oxidation over porous CuCo-based catalysts derived from layered double hydroxide with resistance of water vapor. *Appl Catal B Environ* 2015;166–167:260–9.
- [19] Goto T, Fu Z, Zhang L. Preparation of Layered Double Hydroxide and its Graphene Composite Films as Electrodes for Photoelectrochemical Cells. *Key Eng Mat* 2015;616:129-33.
- [20] Li Y, Zhang L, Xiang X, Yan D, Li F. Engineering of ZnCo-layered double hydroxide nanowalls toward high-efficiency electrochemical water oxidation. *J Mater Chem A* 2014;2:13250-8.
- [21] Donnet JB, Bansal RC, Wang MJ. *Carbon Black: Science and Technology*. 2th ed. New York: Marcel Dekker, INC; 1993.
- [22] Tao Q, Reddy BJ, He H, Frost RL, Yuan P, Zhu J. Synthesis and infrared spectroscopic characterization of selected layered double hydroxides containing divalent Ni and Co. *Mater Chem Phys* 2008;112:869-875.
- [23] Abdolmohammad-Zadeh H, Kohansal S. Determination of Mesalamine by Spectrofluorometry in Human Serum after Solid-Phase Extraction with Ni-Al

Layered Double Hydroxide as a Nanosorbent. *J Braz Chem Soc* 2012;23:473-81.

[24] Moon J-S, Jang J-H, Kim E-G, Chung Y-H, Yoo SJ, Lee Y-K. The nature of active sites of Ni₂P electrocatalyst for hydrogen evolution reaction. *J Catal* 2015;326:92-9.

[25] Abbaspour A, Mirahmadi E. Electrocatalytic hydrogen evolution reaction on carbon paste electrode modified with Ni ferrite nanoparticles. *Fuel* 2013;104:575-82.

[26] Dai X, Li Z, Du K, Sun H, Yang Y, Zhang X, Ma X, Wang J. Facile Synthesis of In-Situ Nitrogenated Graphene Decorated by Few-Layer MoS₂ for Hydrogen Evolution Reaction. *Electrochim Acta* 2015;171:72-80.